sciendo
Acta hort regiotec, 25, 2022(2): 160–173
DOI: 10.2478/ahr-2022-0020

Review

# Reviewing the effect of pyrolysis temperature on the fourier-transform infrared spectra of biochars

Narges Hemati Matin[1,2] *, Elena Aydin[2]

[1]*Bu-Ali Sina University, College of Agriculture, Department of Soil Science, Hamadan, Iran*
[2]*Slovak University of Agriculture in Nitra, Faculty of Horticulture and Landscape Engineering, Institute of Landscape Engineering, Slovak Republic*

Article Details: Received: 2022-05-29 | Accepted: 2022-10-13 | Available online: 2022-11-30

Licensed under a Creative Commons Attribution 4.0 International License

SCREENED BY iThenticate® Professional Plagiarism Prevention

Pyrolysis of feedstocks to produce biochar for soil remediation employed to be a convenient method regarding improvement of soil fertility, increasing carbon stability and decreasing greenhouse gas emissions. Biochar properties and its effect after incorporation into the soils vary depending on the characteristics of feedstocks and pyrolysis process. This paper aims to compare the effect of pyrolysis temperature on the frequency of functional groups in different biochars made from plant feedstocks over the temperature range from 300 °C to 700 °C. An increase in pyrolysis temperature positively affects biochar surface properties until the deformation step in C = O, –COOH, and OH groups and as a result, the surface area of biochar decreases at high temperature (more than 600 °C). The breakdown of hemicellulose, cellulose, and lignin also occurs at temperatures more than 600 °C. Consequently, the biochar quality is reduced with increasing pyrolysis temperature although such biochar may be suitable for rising the content of stable carbon in the soils. Over the long-term, the stability of biochar can contribute to carbon sequestration, retention of water and ions in the soil.

**Keywords:** pyrolysis temperature, carbonization, degradation, functional groups

## 1 Introduction

Biochar is a valuable, carbon-rich material produced from organic residues using pyrolysis process (Ali et al., 2022). This highly porous structure is used as an amendment for sorption of organic and inorganic contaminants (Ambaye et al., 2021). It has been increasingly studied and used as a promising soil amendment also because of high potential of carbon sequestration and soil remediation (Das, Ghosh & Avasthe, 2020). Because of this, the incorporation of biochar into the soil produced in different conditions has become the subject of many research studies in recent years (Uchimiya et al., 2011; Sun et al., 2014; Zhang et al., 2018). The biochar properties after pyrolysis at different temperatures are crucially dependent on the inherent biopolymers and chemical composition of feedstock materials (Kloss et al., 2012; Li et al., 2016). These materials include a wide range of organic materials such as animal and plant-based feedstocks which contain different functional groups (Song et al., 2019). For example, feedstocks of plant origin mostly consist of cellulose, hemicellulose, and lignin, while animal residual feedstocks mostly contain gelatin, collagen, and polysaccharides (Li et al., 2016; Jung et al., 2018).

Moreover, the pyrolysis conditions influence the final properties of produced biochar. These conditions include the type of pyrolysis process (fast, moderate, and slow pyrolysis), temperature degree, and residence time of the material within the reactor (Aghbashlo et al., 2019; Huang et al., 2021). The type of functional groups in biochar present after pyrolysis is an important parameter in choosing the way to produce biochar because these active surfaces affect biochar's quality and function for immobilization and sorption of contaminants. In the study by Van de Velden et al. (2010), cellulose was depolymerized at low temperatures (300–450 °C) and subsequently defragmented at a higher temperature (600 °C); then it was transformed into carboxylic acid,

***Corresponding Author:** Narges Hemati Matin, Bu-Ali Sina University, College of Agriculture, Department of Soil Science, Hamadan, Iran; Institute of Landscape Engineering, Faculty of Horticulture and Landscape Engineering, Slovak University of Agriculture in Nitra, Nitra, Slovakia; e-mail: nargeshmatimatin@gmail.com

alcohol, aldehyde, ketone, and anhydro sugars, etc. The novelty of this study lies in the comparison of the functional groups in biochar made from the same plant feedstocks at different temperatures and described in different studies. The main question was whether application of the same feedstocks from different places will have effect on the peak's intensity and surface properties of biochar or not. The information about FTIR patterns of biochar is still limited and key aspect of collecting biochar FTIR patterns in this study is the ability to quantitatively characterize different feedstocks before starting to produce biochar. As researchers have information about the surface characteristics of produced biochars, they can easily choose best feedstock according to their requirements. Therefore, it can be hypothesized that variation of pyrolysis temperature can affect surface properties of biochars produced from the same feedstocks and the functional groups will change with changes in pyrolysis temperature. The main objective of this paper is to review the published literature and list the important functional groups of biochars produced from plant feedstocks at different pyrolysis temperatures ranging between 300 and 700 °C.

## 2 Biochar definition

Biochar is basically a type of charcoal which is produced intentionally to be used as a soil amendment (Lehmann, Gaunt & Rondon, 2006). Lehmann & Joseph (2015) described biochar as a "carbon-rich product obtained from burning biomass such as wood, manure, and leaves with little or no air". Verheijen et al. (2010) defined biochar as "a primary and stable source of organic carbon produced from heating biomass during pyrolysis at a temperature range of 300 to 1,000 °C in the absence of oxygen." Biochar is also defined as "a heterogeneous carbon material produced by the thermal alteration of different feedstocks comprising a variety of surface functional groups" (Alkurdi et al., 2019). Shackley et al. (2012) had descriptively defined biochar as "a porous organic structure produced by the thermochemical conversion (such as pyrolysis) of organic matter in the absence of oxygen and having convenient physical and chemical properties for long-term storage in the environment." The Biochar International Initiative (IBI) provided a standard definition of biochar, which is "a solid obtained from biomass pyrolysis in an oxygen-restricted environment" (IBI, 2012). All these definitions directly or indirectly refer to the conditions of biochar production and its application in the soils.

### *2.1 Raw materials (feedstocks) for biochar production*

Biomass residues widely employed for biochar production include forest residues (such as Norway pine and Scots poplar), agricultural residues (such as cattle and poultry manures, stems, rice husks, sugar beets, walnut, and almond shells), municipal and household solid residues (such as sewage sludge and food wastes) (Brick & Lyutse, 2010; Cantrell et al., 2012; Carrier et al., 2012; Alburquerque et al., 2014; Khan et al., 2017; Kiran et al., 2017; Griffin et al., 2017). These materials can vary depending on the study area's climate, the availability of organic residues, soil conditions, and economics in these areas. For example, Lehmann & Joseph, (2015) and Alkurdi et al. (2019) noticed that typical biochar was obtained from wood, leaves, manure, municipal waste sludge in their studied areas. Ippolito et al. (2020) reported straws and biosolids, poultry, cattle, and dairy manure as the most common feedstocks to produce biochar. As previously mentioned, these selected feedstocks were generally pyrolyzed in an instrument in the presence of low or without oxygen and the detailed information of pyrolysis process published in the investigated literature in this study is presented in section 3.

### *2.2 Positive effects of biochar application to soil*

The number of articles published about biochar and its application into the soils has significantly increased from 2010 to 2021 which indicates an increasing attention to the use of biochar in scientific research. Because of the porous structure, specific surface area, and large micro-pores, biochar has many beneficial effects on the soil (Cao et al., 2009; Ahmad et al., 2014). Since biochar is a rich source of stable organic carbon, its incorporation benefits the soils by slowing down a reduction in mineralization rate of dissolved organic carbon and an increase of carbon stability in the soils (Amonette et al., 2003; Spokas et al., 2009). Therefore, in order to enhance carbon storage and improve soil fertility, it is necessary to use materials that have the ability to supply energy from organic residues through mechanical or physical, thermochemical, and biological processes. Significant increases were observed in microbe population and activities, seed's germination, stable carbon, plant growth and yields in soils treated with biochar (Verheijen et al., 2010). Besides, the progressive biochar application positively influenced soil physical properties and greenhouse gas emissions which was investigated in different studies (Mukherjee & Lal, 2013; Toková et al., 2020; Horák et al., 2020). However, Blanco-Canqui (2021) and Regmi et al. (2022) have concluded that biochar application can have negative and neutral effect on soil physical and chemical properties.

Biochar has also been considered as an environmentally friendly remediator in recent years (Ahmad et al., 2016; Abbas et al., 2018a; Abbas et al., 2018b). It has been proved in different studies that using biochar derived

from different raw materials can be widely employed to sorb organic and inorganic contaminants like potentially toxic elements (Xu et al., 2019), pesticides (Herath et al., 2016) and pharmaceuticals (Zeng et al., 2019) that are detected in soils and water surfaces (Alkurdi et al., 2019). The biochar adsorption capacity can affect the important surface properties of the final product such as porosity, surface area, and pore size (Ambaye et al., 2021). FTIR spectroscopy is a common technique for qualitative surface analysis of biochar in the laboratory (Yaashikaa et al., 2020). Since the combination of each material is unique, its FTIR pattern is absolutely independent from other samples such as a fingerprint. It is used to determine infrared absorption peaks of samples according to the frequencies of vibrations between the bonds of the atoms producing material. The intensity, size, and number of peaks in specific wavenumber show a group of atoms in an organic molecule nominating functional groups such as alkanes, alcohols, carboxyl, and ketones. The reactivity of functional groups depends on their origins, bonds, and compounds (C, O, and H). Biochar as a material containing functional groups has a lot of positive effects to the soils like ion adsorption (Rao, 2021). In particular, carboxyl, hydroxyl, and phenolic groups on biochar surfaces bond well with soil contaminants (Uchimiya et al., 2011). Also, functional groups improved bioavailability of high-consumption elements such as phosphorus and nitrogen (Dai et al., 2018; Bornø, Müller-Stöver & Liu, 2018). However, increasing temperature during biochar production could selectively remove oxygen from functional groups because of the oxidation process and subsequently cause the decomposition of some of functional groups and reduce the specific surface area of biochar (Hou et al., 2022). As mentioned, this work focused on how pyrolysis temperatures affect biochar surface properties and how the intensity of peaks corresponds to the functional groups in FTIR patterns.

## 3 FTIR of biochar

In this study, the FTIR spectra were extracted from 25 literature sources to compare the effect of temperature on the peak intensity and the frequency of biochar functional groups. Feedstocks data included biochars made from the straws, sugarcane bagasse, manures, shells, and wood chips, etc. Temperature pyrolysis of these studies ranged between 300 to 700 °C for 1–4 h. The detailed FTIR measurement depends on the study purpose and the properties of available instruments, and it may vary in different studies. For instance, in a study by Matin et al. (2020), the FTIR spectra of biochar produced from walnut and almond shells was measured by 2 mg of ground biochar using a ceramic source of infrared and a potassium bromide (KBr) beam splitter which scanned sample in wavenumbers from 4.0 to 40.0 $m^{-1}$ in an average of 10 scans at 0.01 $m^{-1}$ – intervals with a resolution of 0.04 $m^{-1}$. For FTIR measurement, some infrared radiation was absorbed and some of it transmitted from biochar samples. The result of spectrum was presented as the sample absorbance and transmission in a graphical figure such as Fig. 1. In this figure, the fluctuation absorbance of almond shell and its produced biochar at different temperatures was detected in FTIR spectra (Liu, He & Uchimiya, 2015).

There are organic functional groups on the surface of biochar, which can sorb ions to form surface complexes by biochar surfaces (Godwin et al., 2019). The main active functional groups with the wavenumber ($m^{-1}$) in different studies used for the purposes of this review are listed in Table 1. One of the important functional groups which is assigned in the most FTIR spectra of biochar is O–H stretching known as hydroxyl bond at about 34.0 $m^{-1}$ wavenumbers. These wavenumbers might vary from one feedstock to another and depend on the conditions of biochar production process but the results of FTIR patterns are comparable.

The differences of wavenumbers and functional groups of some biochar produced from straws are shown in Table 2. There is a peak at 34.9 $m^{-1}$ for rice and wheat straws related to OH

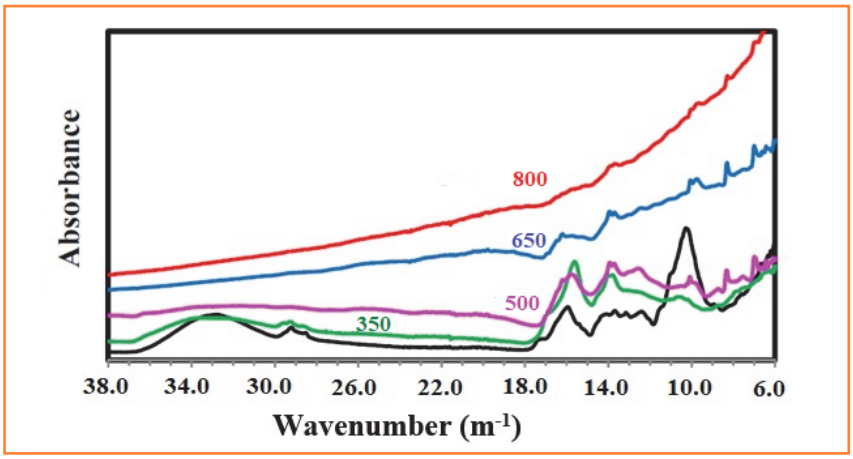


**Figure 1** FTIR patterns of almond shell and biochar-derived almond shell at 350, 500, 650, and 800 °C temperatures. Black line shows almond shell FTIR spectra
Source: Liu, He & Uchimiya, 2015

**Table 1** The main active functional groups identified in the biochar surface.

| Wavenumber ($m^{-1}$) | Functional group |
|---|---|
| **36.0–32.0** | O–H stretching (water, hydrogen-bonded hydroxyl) |
| **29.3–28.5** | C–H stretching (aliphatic CHx) |
| **17.4–17.0** | C = O stretching (carboxyl and ketones) |
| **16.3–16.0** | C = C stretching of aromatic components or C = O stretching (quinones and ketonic acids) |
| **14.4** | C = C stretching of aromatic C |
| **13.75** | aliphatic deformation of $CH_2$ or $CH_3$ groups or O–H bending (phenolic–OH) |
| **13.25** | O–H bending (phenols, phenolic; ligneous syringyl) |
| **11.1–10.3** | C–O–C stretching vibrations (cellulose and hemicellulose) |
| **9.0–7.5** | C–H bending aromatic CH |
| **8.85** | C–H bending (aromatic C–H out-of-plane deformation) |
| **7.81** | Pyridine (pyridine ring vibration and C–H deformation) |

References: Yaman, (2004); Das et al. (2009); Özçimen & Ersoy-Meriçboyu, (2010); Uchimiya et al. (2011); Cantrell et al. (2012); Ahmad et al. (2012); Claoston et al. (2014)

stretching vibration which is identified as alcoholic and phenolic functional groups (Sahoo, Kumar & Chakraborty, 2021). Sahoo, Kumar & Chakraborty (2021) reported that C–H stretching vibration in rice and wheat straws at 29.1 $m^{-1}$ (or 29.3 $m^{-1}$) confirmed various carbohydrate monomers and alkanes in three studied straws which was similar to other studies (Pütün et al., 2005; Apaydin-Varol, Pütün & Pütün, 2007; Yuan, Xu & Zhang, 2011). The peak at 21.40 $m^{-1}$ indicated an alkyne group in rice and wheat samples (Yang et al., 2007). Tong et al. (2011) reported –COO– deviational vibration and symmetric stretching at 7.79 or 7.83 $m^{-1}$ assigned for canola, peanut, and soybean straw (Fu et al., 2009; Lammers, Arbuckle-Keil & Dighton, 2009). Tong et al. (2011) also observed a peak at 15.81 $m^{-1}$ for –COOH identified as anti-symmetric for these straws. But these peaks showed small changes in corn, soybean, and canola straws as reported by Yuan, Xu & Zhang (2011) at 14.3, 15.9, and 34.0 $m^{-1}$ for three studied straws. Yuan, Xu & Zhang (2011) reported peaks at 10.6 and 16.0 $m^{-1}$ for corn, soybean, and canola straws identified to the straight chain C–C stretching (or sugar C–OH stretching), –COO– antisymmetric stretching of amino acids, respectively (Table 2). Some studies have investigated the effect of fast and slow pyrolysis on biochar quality (Huang et al., 2008; Septien et al., 2012; Lin et al., 2017) and they observed that biochar produced by fast pyrolysis was more reactive and porous than biochar made by slow pyrolysis (Zanzi, Sjöström & Björnbom, 1996). However, the cost of biochar production by slow pyrolysis is lower when compared to fast pyrolysis (Kung, McCarl & Chen, 2014). Fastly pyrolyzed biochar contained more oxygen in various functional groups, not just alkyl C–OH as the feedstock. The somewhat enhanced COO concentration in biochar produced by fast pyrolysis may actually result in a slightly better cation exchange capacity (Brewer et al., 2009).

In comparison to other studies, Wu et al. (2012) observed the aliphatic C–H, C–O stretching, and C–O–C skeletal vibrations in pyranose ring in rice straw contributing to 29.5 or 28.5, 11.1–10.3 and 10.8 $m^{-1}$ wavenumbers at 300 °C (Table 2). Sahoo, Kumar & Chakraborty (2021) observed that the peak at 14.4 $m^{-1}$ in rice and wheat straws indicated methoxy functional group with $O–CH_3$ formula which is the basic structure of phenyl propane of lignin. The average intense peak at 17.2 $m^{-1}$ for rice and wheat indicated C = O stretching vibration which assigned to the quinone, aldehyde and ketonic functional groups (Pütün et al., 2005; Apaydin-Varol, Pütün & Pütün, 2007; Sahoo, Kumar & Chakraborty, 2021). The presence of alkenes and aromatic functional groups in two straws shown at 16.2 $m^{-1}$ peak confirms the association of C = C stretching vibration with lignin (Pütün et al., 2005). An intense peak at 6.94 $m^{-1}$ in rice straw biochar confirmed the existence of mono-, polycyclic, and substituted aromatic compounds related to the basic structure of lignocellulosic components in organic wastes (Asadullah et al., 2013; Sahoo, Kumar & Chakraborty, 2021). An exception for peanut straw was observed in the 10.3 $m^{-1}$ peak contributing to Si–O stretching in comparison to other straws that indicated the presence of SiO2 in peanut straw. This broad peak covered two peaks of 11.0 and 8.6 $m^{-1}$ at 700 °C, and consequently both peaks disappeared from the FTIR pattern of peanut (Yuan, Xu & Zhang, 2011).

The pattern of biochar functional groups exhibited the characteristics of the raw materials and the procedures used to produce them such as particles' sizes, pyrolysis temperature, residence time (Janu et al., 2021). The impact

of different pyrolysis temperatures on the FTIR patterns of biochars in some studies showed that the total functional groups dropped with increasing pyrolysis temperature in the same biomass. This was confirmed in some studies in which biochar was produced from different straws (Table 2) (Tong et al., 2011; Yuan, Xu & Zhang, 2011; Wu et al., 2012; Trazzi et al., 2016; Sahoo, Kumar & Chakraborty, 2021). For example, the effect of an increase in pyrolysis temperature was observed at approximately 34.0 $m^{-1}$ peak where its intensity decreased in rice straw, suggesting an ignition loss of OH at the high temperature of these studies. With temperature rises in a study by Wu et al. (2012), the bond intensity of aliphatic C–H stretching (29.5–28.5 $m^{-1}$) dropped, but bonds arising from aromatic C–H out of plane vibrations (7.0–9.0 $m^{-1}$) became more apparent in rice straw.

A peak at 7.8 $m^{-1}$ was detected in the FTIR spectra of peanut straw biochar at 300 and 500 °C temperatures in the study by Yuan, Xu & Zhang (2011), but it disappeared at 700 °C. As the biochar made from corn, soybean, and canola straws had the same functional groups, the intensities of their peaks changed when pyrolysis temperature increased (Chen, Zhou & Zhu, 2008; Yuan, Xu & Zhang, 2011; Tong et al., 2011). The peak intensity of the C = O functional group (17.0 and 17.3 $m^{-1}$) for rice and wheat straws became narrow and vanished with an increase in the temperature. This can be explained by the emission of CO and $CO_2$ gases and degradation of C = O bond (Sahoo, Kumar & Chakraborty, 2021). The same authors observed another interesting fact in C–O (14.5 and 10.8 $m^{-1}$) and CH aromatic ring (14.4 and 8.9 $m^{-1}$), which were enhanced because of reducing OH and CH alkyl groups with an increase in temperature. But when temperature increased to about 650 °C, the intensity of the peak declined. There is evidence that aromatic functional groups re-polymerized and $H_2$ gas emission increased at 600 °C temperature (Yang et al., 2007; Yuan, Tahmasebi & Yu, 2015). The degradation of hemicellulose and cellulose which are the main components of rice straw is much faster than lignin during pyrolysis process (Yang et al., 2007). It may cause weight loss and reduction of H/C, O/C ratios in this straw rather than other kinds of feedstock's texture such as wood or grass under the same pyrolysis condition (Keiluweit et al., 2010). An extensive loss of active functional groups and significant precipitation of aromatic structures was reported at all wavenumbers at temperature up to 750 °C (Mochidzuki et al., 2003; Huang et al., 2021). The impact of higher pyrolysis temperatures was tested in a study by Dieguez-Alonso et al. (2018) and they concluded that thermal stability of biochar increased because of the increasing resistance against microbiological degradation. The amount of –COOH as acidic functional groups in wheat straws dropped and vanished with increasing temperature (Chun et al., 2004). This can be due to an increase in biochar pH and the formation of oxide, hydroxide, and carbonate of minerals with rising pyrolysis temperature (Novak et al., 2009).

Moreover, changes in FTIR patterns were detected in biochars with various parent feedstocks when temperature increased during pyrolysis (Table 3). In a study by Sun et al. (2011) and Trazzi et al. (2016), the vibrations assigned in the spectra pattern of sugarcane bagasse at 29.16, 16.99, 15.95, 10.3, 8.2 $m^{-1}$ wavenumbers represented methyl C–H stretching compounds, aromatic carbonyl/carboxyl C = O, aromatic C = C and C = O, aliphatic C–O–C and alcohol–OH, and aromatic C–H, respectively. The functional groups of 10.0 $m^{-1}$ are generally detected in alcoholic and polysaccharide C–O stretching, silicate and phosphate groups (He & Ohno, 2012). In the FTIR pattern of pecan shells, there was a peak at 17.4 $m^{-1}$ attributable to carboxyl C = O groups (Liu, He & Uchimiya, 2015). For the in-wood chips, invasive plant water hyacinth and chicken manure, the peaks of 29.3, 16.2, 14.3, 11.1, and 8.7 or 9.0 $m^{-1}$ were related to the alkyl/aliphatic C–H stretching, aromatic C–C ring stretching, C–H alkanes, C–O–C symmetric stretching and aromatic C–H groups, respectively (Huang et al., 2021). A peak of 16.0 $m^{-1}$ of the C = C bond was observed in a study on wood and grass biochars by Keiluweit et al. (2010). Janu et al. (2021) studied functional groups of biochars produced from 12 raw materials (rice husk, wheat straw, corn cobs, Miscanthus sinensis stems, sunflower stems, cherry stones, walnut shells, biogas digestate, sunflower husks, chicken manure pellets, poplar (*Populus nigra* L.) wood chips and conifer (*Picea abies* L.) wood chips) at four temperatures (300, 450, 600, and 750 °C) and reported that at the low to medium pyrolysis temperature range (300–600 °C), two peaks at 36.3 $m^{-1}$ and 30.6 $m^{-1}$ were observed for free O-H stretching of phenolic and alcoholic -OH and C-H stretching of substituted aromatic C functional groups, respectively. Similar aromatic compounds including C = C, C = O, and C–On bonds were observed in the structure of biochar produced from the sugarcane bagasse, eucalyptus (*Eucalyptus globulus*) bark, and sewage sludge with peaks of 36.0, 23.6, 17.0, 16.0, 13.0, 12.0, and 10.3 $m^{-1}$ (Figueredo et al., 2017) (Table 3). For sewage sludge biochar at 500 °C, the peak of O–H bonds from 37.0 to 36.0 $m^{-1}$ was identified in the study by Figueredo et al. (2017).

Zolfi Bavariani, Ronaghi & Ghasemi (2019) reported that the peaks at 34.0 $m^{-1}$ and 29.7 $m^{-1}$ for poultry manure biochar decreased with rising temperature from 200 to 500 °C. The wavenumber at 34.2 $m^{-1}$ was observed in the biochar produced from wood chips, invasive plant water hyacinth and chicken manure at both 300 or 600 °C

**Table 2** The main functional groups of some biochars produced from different straws

| Biochar | T (°C) | I ($m^{-1}$) | –OH | COH | II | C–O | III | C = O | C = C | References |
|---|---|---|---|---|---|---|---|---|---|---|
| **Canola straw** | 300 | 7.8, 14.0, 15.9 | 34.0 | 14.3 | – | – | 29.3 | – | 10.6 | Yuan, Xu & Zhang (2011) |
| | 400 | 7.8, 14.1, 15.8 | 34.06 | – | – | – | – | – | – | Tong et al. (2011) |
| | 500 | 14.0, 15.9 | 34.0 | 14.3 | 8.6, 11.0 | – | 29.3 | – | 10.6 | Yuan, Xu & Zhang (2011) |
| | 700 | – | 34.0 | 14.3 | 8.6, 11.0 | – | 29.3 | – | 10.6 | Yuan, Xu & Zhang (2011) |
| **Corn straw** | 300 | 7.8, 14.0, 15.9 | 34.0 | 14.3 | – | – | 29.3 | – | 10.6 | Yuan, Xu & Zhang (2011) |
| | 500 | 14.0, 15.9 | 34.0 | 14.3 | 8.6, 11.0 | – | 29.3 | – | 10.6 | Yuan, Xu & Zhang (2011) |
| | 700 | – | 34.0 | 14.3 | 8.6, 11.0 | – | 29.3 | – | 10.6 | Yuan, Xu & Zhang (2011) |
| **Soybean straw** | 300 | 7.8, 14.0, 15.9 | 34.0 | 14.3 | – | – | 29.3 | – | 10.6 | Yuan, Xu & Zhang (2011) |
| | 400 | 7.8, 14.1, 15.8 | 34.14 | – | – | – | – | – | – | Tong et al., 2011 |
| | 500 | 14.0, 15.9 | 34.0 | 14.3 | 8.6, 11.0 | – | 29.3 | – | 10.6 | Yuan, Xu & Zhang (2011) |
| | 700 | – | 34.0 | 14.3 | 8.6, 11.0 | – | 29.3 | – | 10.6 | Yuan, Xu & Zhang (2011) |
| **Peanut straw** | 300 | 7.8, 14.0, 15.9 | 34.0 | 14.3 | – | – | 29.3 | – | 10.6 | Yuan, Xu & Zhang (2011) |
| | 400 | 14.1, 15.8 | 34.14 | – | – | – | – | – | – | Tong et al. (2011) |
| | 500 | 7.8, 14.0, 15.9 | 34.0 | 14.3 | 8.6, 11.0 | – | 29.3 | – | 10.6 | Yuan, Xu & Zhang (2011) |
| | 700 | – | 34.0 | 14.3 | 8.6, 11.0 | – | 29.3 | – | 10.6 | Yuan, Xu & Zhang (2011) |
| **Rice straw** | 300 | – | 32.0-36.0 | 10.8 | 10.3–11.1 | – | 7.5–9.0, 28.5–29.5 | 17.0–17.4 | 16.0–16.3 | Wu et al. (2012) |
| | 350 | 6.9 | 34.9 | 14.4 | – | – | 29.1 | 17.2 | 16.2 | Sahoo, Kumar & Chakraborty (2021) |
| | 550 | – | – | – | – | 14.5, 10.8 | 8.9, 14.4, 28.6, 29.7 | – | – | Sahoo, Kumar & Chakraborty (2021) |
| | 650 | – | – | – | – | 14.5, 10.8 | 8.9, 14.4, 28.6, 29.7 | – | – | Sahoo, Kumar & Chakraborty (2021) |
| **Wheat straw** | 350 | 6.9 | 34.9 | 14.4 | – | – | 29.1 | 17.2 | 16.2 | Sahoo, Kumar & Chakraborty (2021) |
| | 550 | – | – | – | – | 14.5, 10.8 | 8.9, 14.4, 28.6, 29.7 | – | – | Sahoo, Kumar & Chakraborty (2021) |
| | 650 | – | – | – | – | 14.5, 10.8 | 8.9, 14.4, 28.6, 29.7 | – | – | Sahoo, Kumar & Chakraborty (2021) |

T: temperature; I: –COO– and –COOH; II: C-O-C, C( = O)([O-])[O-]; III: C–H stretching and aromatic rings

**Table 3a** The main functional groups of some biochars produced from different plant residues

| Biochar | T | I | –OH | –COH | II | C–O | III | H–C = C–H | C = O | C = C | References |
|---|---|---|---|---|---|---|---|---|---|---|---|
| | (°C) | ($m^{-1}$) | | | | | | | | | |
| Sugarcane bagasse | 350 | 6.94 | 34.9 | 14.4 | – | – | 29.1 | – | 17.2 | 16.2 | Sahoo, Kumar & Chakraborty (2021) |
| | 550 | – | – | – | – | 14.5, 10.8 | 8.9, 14.4, 28.6, 29.7 | – | – | – | Sahoo, Kumar & Chakraborty (2021) |
| | 650 | – | – | – | – | 14.5, 10.8 | 8.9, 14.4, 28.6, 29.7 | 21.40 | – | – | Sahoo, Kumar & Chakraborty (2021) |
| | 300 | 8.15 | – | 14.4 | 10.3 | – | 29.16 | – | 16.99 | 15.95 | Trazzi et al. (2016) |
| | 500 | 8.15 | – | 14.4 | – | – | – | – | 16.99 | 15.95 | Trazzi et al. (2016) |
| | 700 | 8.15 | – | – | – | – | – | – | – | 15.95 | Trazzi et al. (2016) |
| | 350 | – | 36.0 | – | 10.3 | 10.0-13.0 | 10.0-13.0 | – | 17.0-17.4 | 14.75-16.0 | Figueredo et al. (2017) |
| | 500 | – | 36.0 | – | 10.3 | 10.0-13.0 | 10.0-13.0 | 23.0 | 17.0-17.4 | 14.75-16.0 | Figueredo et al. (2017) |
| 12 raw materials† | 300–750 | – | 34.5, 36.3 | – | 10.5, 11.2 | – | 28.7, 30.6 | – | 23.6 | 14.75, 16.1 | Janu et al. (2021) |
| Eucalyptus bark | 350 | – | – | – | – | – | – | 23.0 | 24.0 | 14.75-16.0 | Figueredo et al. (2017) |
| | 500 | – | – | – | – | – | – | 23.0 | 24.0 | 14.75-16.0 | Figueredo et al. (2017) |
| Sewage sludge | 350 | – | 36.0-37.0 | – | – | 10.0 | – | – | 24.0 | 16.0 | Figueredo et al. (2017) |
| | 500 | – | 36.0-37.0 | – | – | 10.0 | – | – | 240 | 16.0 | Figueredo et al. (2017) |

T: temperature; I: –COO– and –COOH; II: C-O-C, C( = O)([O-])[O-]; III: C–H stretching and aromatic rings. † Rice husk, wheat straw, corn cobs, Miscanthus sinensis stems, sunflower stems, cherry stones, walnut shells, biogas digestate, sunflower husks, chicken manure pellets, poplar (*Populus nigra* L.) wood chips and conifer (*Picea abies* L.) wood chips

**Table 3b** The main functional groups of some biochars produced from different plant residues

| Biochar | T | II | –OH | –COH | C–O | III | H–C = C–H | C = O | C = C | | References |
|---|---|---|---|---|---|---|---|---|---|---|---|
| | (°C) | ($m^{-1}$) | | | | | | | | | |
| **Almond shell** | 350 | – | 32.8 | 14.0 | – | 10.3 | 29.2, 28.5 | – | 17.3 | 16.0 | Liu, He & Uchimiya (2015) |
| | 500 | 7.0, 8.3 | – | 14.0 | – | 10.3 | – | – | 16.0 | 16.0 | Liu, He & Uchimiya (2015) |
| | 650 | – | – | – | – | – | – | – | – | 16.0 | Liu, He & Uchimiya (2015) |
| | 800 | – | – | – | – | – | – | – | – | – | Liu, He & Uchimiya (2015) |
| **Pecan shell** | 400 | 8.7 | 34.0 | 14.0 | – | | 29.2, 28.5 | | 17.4 | 16.0 | Liu, He & Uchimiya (2015) |
| | 500 | – | – | – | – | – | – | – | – | 16.0 | Liu, He & Uchimiya (2015) |
| | 600 | – | – | – | – | – | – | – | – | – | Liu, He & Uchimiya (2015) |
| | 700 | – | – | – | – | – | – | – | – | – | Liu, He & Uchimiya (2015) |
| **Cottonseed hull** | 350 | 7.0-9.0 | 34.0 | 14.0 | – | 10.26 | 29.2, 28.5 | – | 17.3 | 16.0 | Liu, He & Uchimiya (2015) |
| | 500 | 7.0, 8.3 | – | 14.0 | – | 10.26 | – | – | 16.0 | 16.0 | Liu, He & Uchimiya (2015) |
| | 650 | – | – | – | – | – | – | – | – | 16.0 | Liu, He & Uchimiya (2015) |
| | 800 | – | – | – | – | – | – | – | – | – | Liu, He & Uchimiya (2015) |
| **Broiler litter** | 350 | 9.7 | 32.8 | 14.0 | – | 10.25 | 29.0 | – | 16.4 | 16.0 | Liu, He & Uchimiya (2015) |
| | 500 | 9.7 | – | – | – | 10.25 | – | – | – | – | Liu, He & Uchimiya (2015) |
| | 650 | 9.7 | – | – | – | 10.25 | – | – | – | – | Liu, He & Uchimiya (2015) |
| | 800 | 9.7 | – | – | – | 10.25 | – | – | – | – | Liu, He & Uchimiya (2015) |

T: temperature; I: –COO– and –COOH; II: C-O-C, C( = O)([O-])[O-]; III: C–H stretching and aromatic rings

**Table 3c** The main functional groups of some biochars produced from different plant residues

| Biochar | T | I | –OH | –COH | C–O | III | H–C = C–H | C = O | C = C | | References |
|---|---|---|---|---|---|---|---|---|---|---|---|
| | (°C) | ($m^{-1}$) | | | | | | | | | |
| **Apple tree branches** | 300 | 7.8 | 34.0 | 13.3 | – | 10.3-11.1 | 29.4 | – | 16.0 | 14.4 | Zhao, Ta & Wang (2017) |
| | 400 | 7.8 | 34.0 | 13.3 | – | – | | – | 16.0 | 14.4 | Zhao, Ta & Wang (2017) |
| | 500 | – | 34.0 | – | – | – | 8.9 | – | 16.0 | 14.4 | Zhao, Ta & Wang (2017) |
| | 600 | – | 34.0 | – | – | – | 8.9 | – | 16.0 | 14.4 | Zhao, Ta & Wang (2017) |
| **Poultry manure** | 200–500 | – | 34.0 | – | – | – | 29.7 | – | 10.5, 12.5 | 15.0–16.7 | Zolfi Bavariani, Ronaghi & Ghasemi (2019) |
| **Wood chips** | 300 | – | 34.2 | 14.3 | | 11.1 | 29.3 | – | – | 16.2 | Huang et al. (2021) |
| | 600 | – | 34.2 | – | – | – | – | – | – | 16.2 | Huang et al. (2021) |
| **Plant water hyacinth** | 300 | – | 34.2 | – | – | 11.1 | 8.7, 29.3 | – | – | 16.2 | Huang et al. (2021) |
| | 600 | – | 34.2 | 14.3 | – | 11.1 | 8.7, 29.3 | – | – | 16.2 | Huang et al. (2021) |
| **Chicken manure** | 300 | – | 34.2 | 14.3 | – | 11.1 | 8.7, 29.3 | – | – | 16.2 | Huang et al. (2021) |
| | 600 | – | 34.2 | 14.3 | – | 11.1 | 8.7, 29.3 | – | – | 16.2 | Huang et al. (2021) |

T: temperature; I: –COO– and –COOH; II: C–H stretching and aromatic rings

temperatures (Huang et al., 2021). This is in agreement with some other researchers that these organic O–H groups are very unstable at elevated temperatures and cause accelerating the dehydration reaction of biomass (Chen, Chen & Lv, 2011; Hossain et al., 2010). The peak intensity from 17.0 to 17.4 $m^{-1}$ and 16.0 to 14.8 $m^{-1}$ at 350 °C for poultry manure biochar were greater than at 500 °C and a peak of 23.0 $m^{-1}$ was assigned at 500 °C. In addition to carboxylic acid, ketone, alcohol which was similar to sugarcane bagasse, ether and phenol groups were observed in sewage sludge biochar, but the ketone group was only detected in eucalyptus bark biochar (Figueredo et al., 2017). The polar functional groups including hydroxyl and C–O showed the lower noticeable peaks during pyrolysis at high temperature (500 and 700 °C). The absence of carboxyl (–COO–) and hydroxyl (–OH) in wood chips, invasive plant water hyacinth and chicken manure was clearly detected at high pyrolysis temperature (Huang et al., 2021).

Along with the earlier observations, it was illustrated that the intensity of peaks decreased in almond shell, pecan shell, broiler litter, and cottonseed hull biochars with increasing pyrolysis temperature from 350 to 500 °C. In the study by Liu, He & Uchimiya (2015), different peaks at 32.8, 29.2, 28.5, 17.3, 10.3 $m^{-1}$ dropped with a temperature pyrolysis increase. In contrast, there were some bonds in the FTIR at which the intensity increased including the 8.3, 7.0, and 14.0 $m^{-1}$ (Liu, He & Uchimiya, 2015). The carbonyl and carboxyl groups in carbohydrates at 16.7, 12.0, and 10.0 $m^{-1}$ in poultry manure also gradually diminished and disappeared at 500 °C (Zolfi Bavariani, Ronaghi & Ghasemi, 2019). Uchimiya et al. (2013) reported an intense vibration at 43.9 $m^{-1}$ in the cottonseed hull which was a function of fixed C content at high temperature that could indicate an upward baseline shift. The peak of protein carboxyl C = O groups at 16.35 $m^{-1}$ was more pronounced in broiler litter than other biochars studied by Liu, He & Uchimiya (2015). An exception in increase and stability of a peak in poultry manure biochar with an increase in temperature was observed at 16.4 $m^{-1}$ what is related to the existence of plenty of polyphenols (Lin et al., 2007; Zolfi Bavariani, Ronaghi & Ghasemi, 2019).

In a study by Zhao, Ta & Wang (2017) on biochar produced from apple tree branches at varying pyrolysis temperatures ranging between 300 to 600 °C, the peak intensities at 13.3 $m^{-1}$ and 16.0 $m^{-1}$ declined with temperature due to the decomposition of phenolic and carboxylic compounds. The highest loss was observed at 600 °C when –OH, $–CH_2$, and C–O functional groups because of the temperature effect while low polar functional groups of –OH and C–O were obtained at 300 °C. A similar behaviour was observed for all 10 tested biochars in the study by Janu et al. (2021) as the biochars were losing functional groups when the temperature was increased in the pyrolysis process. With increasing temperature, the aromatic C and aliphatic $CH_2$-groups observed at 14.0 to 15.0 $m^{-1}$ associated with lignin which is more sustainable than aromatic groups in aldehydes and ketones at 16.0 to 17.0 $m^{-1}$ (Janu et al., 2021). The intensity of functional groups decreased as the temperature arose to >600 °C, but an exception was detected at 10.8 $m^{-1}$ for C–O stretching which was still stable even at 700 °C. The existence of pyranose rings and guaiacyl monomers of cellulose and hemicellulose is a good reason for creating these peaks at high temperature (Lee et al., 2010; Keiluweit et al., 2010; Uchimiya et al., 2011). Biochars are still contributing a high amount of O-contained functional groups but have a tendency to make graphene-like structure with progressive pyrolysis temperature. A reduction of acidic functional groups causes an increase of pH and carbon stability in final biochar as a result of rising temperature. The main reasons for carbon stability are the formation of graphene-C containing higher graphene-like structures and the facility of decomposition which led to non-aromatic degradation vibrations (Wu et al., 2012). Declining biochar yield and enhancing ash content, CEC, and surface area can result from the increase in pyrolysis temperature (Meng et al., 2013; Sun et al., 2014; Alkurdi et al., 2019). Moreover, the C/N ratio of biochar increased with increasing pyrolysis temperature which shows a faster reduction in N content than C, and it causes a drop in nitrogen-containing functional groups (Chen et al., 2014; Zhang et al., 2022).

## 4 Conclusions

Carbonization is a process that involves an increase in aromatic structures and polymerization of organic matters and may also contribute to forced metal sorption in the biochar structure. The persistence of biochar in the environment for a long time due to its polycyclic aromatic structure is a point to be considered in research studies. Various studies have revealed that the quality and functional groups of biochar greatly depended on pyrolysis temperature. Also, there were no specific differences between the peaks of functional groups in the same feedstocks. The carbonyl and carboxyl groups are the most common active groups in biochar produced at low and medium temperatures (300 to 500 °C). Further, the loss of functional groups was repeatedly reported in studied biochars produced at the high temperature (more than 600 °C) and this process continued to the dominance of graphitic C. A good point of increasing pyrolysis temperature over 500 °C is promoting the stability of biochar to long-lasting carbon with more

than 1,000-year half-live. This knowledge could be useful to optimize the pyrolysis process for biochar production according to the purpose of each study such as high sorption ability or carbon sink stability in soil. It can contribute to evaluation of feedstocks before starting the projects and account the active functional groups of produced biochar according to the various literature sources.

**Acknowledgements**

This research was funded by the Scientific Grant Agency, grant number VEGA 1/0747/20, the Slovak Research and Development Agency under the contract No. APVV-21-0089 and Cultural and Educational Grant Agency, grant number KEGA 019SPU-4/2020. Further, this publication is the result of the project implementation "Sustainable smart farming systems, taking into account the future challenges 313011W112", co-financed by the European Regional Development Fund.

## References

Abbas, T., Rizwan, M., Ali, S., Adrees, M., Mahmood, A., Zia-ur-Rehman, M., Ibrahim, M., Arshad, M., & Qayyum, M. F. (2018a). Biochar application increased the growth and yield and reduced cadmium in drought stressed wheat grown in an aged contaminated soil. *Ecotoxicology and Environmental Safety*, 148, 825–833. https://doi.org/10.1016/j.ecoenv.2017.11.063

Abbas, T., Rizwan, M., Ali, S., Adrees, M., Zia-ur-Rehman, M., Qayyum, M. F., Ok, Y. S., & Murtaza, G. (2018b). Effect of biochar on alleviation of cadmium toxicity in wheat (*Triticum aestivum* L.) grown on Cd-contaminated saline soil. *Environmental Science and Pollution Research*, 25(26), 25668–25680. https://doi.org/10.1007/s11356-017-8987-4

Aghbashlo, M., Tabatabaei, M., Nadian, M. H., Davoodnia, V., & Soltanian, S. (2019). Prognostication of lignocellulosic biomass pyrolysis behavior using ANFIS model tuned by PSO algorithm. *Fuel*, 253, 189–198. https://doi.org/10.1016/j.fuel.2019.04.169

Ahmad, M., Lee, S. S., Dou, X., Mohan, D., Sung, J. K., Yang, J. E., & Ok, Y. S. (2012). Effects of pyrolysis temperature on soybean stover-and peanut shell-derived biochar properties and TCE adsorption in water. *Bioresource Technology*, 118, 536–544. https://doi.org/10.1016/j.biortech.2012.05.042

Ahmad, M., Ok, Y. S., Rajapaksha, A. U., Lim, J. E., Kim, B. Y., Ahn, J. H., Lee, Y. H., Al-Wabel, M. I., Lee, S. E., & Lee, S. S. (2016). Lead and copper immobilization in a shooting range soil using soybean stover-and pine needle-derived biochars: Chemical, microbial and spectroscopic assessments. *Journal of Hazardous Materials*, 301, 179–186. https://doi.org/10.1016/j.jhazmat.2015.08.029

Ahmad, M., Rajapaksha, A. U., Lim, J. E., Zhang, M., Bolan, N., Mohan, D., Vithanage, M., Lee, S. S., & Ok, Y. S. (2014). Biochar as a sorbent for contaminant management in soil and water: a review. *Chemosphere*, 99, 19–33. https://doi.org/10.1016/j.chemosphere.2013.10.071

Alburquerque, J. A., Calero, J. M., Barrón, V., Torrent, J., del Campillo, M. C., Gallardo, A., & Villar, R. (2014). Effects of biochars produced from different feedstocks on soil properties and sunflower growth. *Journal of Plant Nutrition and Soil Science*, 177(1), 16–25. https://doi.org/10.1002/jpln.201200652

Ali, L., Palamanit, A., Techato, K., Ullah, A., Chowdhury, M. S., & Phoungthong, K. (2022). Characteristics of biochars derived from the pyrolysis and Co-pyrolysis of rubberwood sawdust and sewage sludge for further applications. *Sustainability*, 14(7), 3829. https://doi.org/10.3390/su14073829

Alkurdi, S. S., Herath, I., Bundschuh, J., Al-Juboori, R. A., Vithanage, M., & Mohan, D. (2019). Biochar versus bone char for a sustainable inorganic arsenic mitigation in water: what needs to be done in future research? *Environment International*, 127, 52–69. https://doi.org/10.1016/j.envint.2019.03.012

Ambaye, T. G., Vaccari, M., van Hullebusch, E. D., Amrane, A., & Rtimi, S. (2021). Mechanisms and adsorption capacities of biochar for the removal of organic and inorganic pollutants from industrial wastewater. *International Journal of Environmental Science and Technology*, 18(10), 3273–3294. https://doi.org/10.1007/s13762-020-03060-w

Amonette, J. E., Kim, J., Russell, C. K., Palumbo, A. V., & Daniels, W. L. (2003, October). *Enhancement of soil carbon sequestration by amendment with fly ash*. In Proceedings.

Apaydin-Varol, E., Pütün, E., & Pütün, A. E. (2007). Slow pyrolysis of pistachio shell. *Fuel*, 86(12–13), 1892–1899. https://doi.org/10.1016/j.fuel.2006.11.041

Asadullah, M., Ab Rasid, N. S., Kadir, S. A. S. A., & Azdarpour, A. (2013). Production and detailed characterization of bio-oil from fast pyrolysis of palm kernel shell. *Biomass and Bioenergy*, 59, 316–324. https://doi.org/10.1016/j.biombioe.2013.08.037

Blanco-Canqui, H. (2021). Does biochar improve all soil ecosystem services? *GCB Bioenergy*, 13(2), 291–304. https://doi.org/10.1111/gcbb.12783

Bornø, M. L., Müller-Stöver, D. S., & Liu, F. (2018). Contrasting effects of biochar on phosphorus dynamics and bioavailability in different soil types. *Science of the Total Environment*, 627, 963–974. https://doi.org/10.1016/j.scitotenv.2018.01.283

Brewer, C.E., Schmidt-Rohr, K., Satrio, J.A., & Brown, R.C. (2009). Characterization of biochar from fast pyrolysis and gasification systems. *Environmental Progress & Sustainable Energy: An Official Publication of the American Institute of Chemical Engineers*, 28(3), 386–396. https://doi.org/10.1002/ep.10378

Brick, S., & Lyutse, S. (2010). *Biochar: Assessing the promise and risks to guide US policy*. Natural Resources Defense Council. USA.

Cantrell, K. B., Hunt, P. G., Uchimiya, M., Novak, J. M., & Ro, K. S. (2012). Impact of pyrolysis temperature and manure source on physicochemical characteristics of biochar. *Bioresource Technology*, 107, 419–428. https://doi.org/10.1016/j.biortech.2011.11.084

Cao, X., Ma, L., Gao, B., & Harris, W. (2009). Dairy-manure derived biochar effectively sorbs lead and atrazine. *Environmental Science and Technology*, 43(9), 3285–3291. https://doi.org/10.1021/es803092k

Carrier, M., Hardie, A. G., Uras, Ü., Görgens, J., & Knoetze, J. H. (2012). Production of char from vacuum pyrolysis of South-African sugar cane bagasse and its characterization as activated carbon and biochar. *Journal of Analytical and Applied Pyrolysis*, 96, 24–32. https://doi.org/10.1016/j.jaap.2012.02.016

Chen, B., Chen, Z., & Lv, S. (2011). A novel magnetic biochar efficiently sorbs organic pollutants and phosphate. *Bioresource Technology*, 102(2), 716–723. https://doi.org/10.1016/j.biortech.2010.08.067

Chen, B., Zhou, D., & Zhu, L. (2008). Transitional adsorption and partition of nonpolar and polar aromatic contaminants by biochars of pine needles with different pyrolytic temperatures. *Environmental Science and Technology*, 42(14), 5137–5143. https://doi.org/10.1021/es8002684

Chun, Y., Sheng, G., Chiou, C. T., & Xing, B. (2004). Compositions and sorptive properties of crop residue-derived chars. *Environmental Science and Technology*, 38(17), 4649–4655. https://doi.org/10.1021/es035034w

Claoston, N., Samsuri, A. W., Ahmad Husni, M. H., & Mohd Amran, M. S. (2014). Effects of pyrolysis temperature on the physicochemical properties of empty fruit bunch and rice husk biochars. *Waste Management and Research*, 32(4), 331–339. https://doi.org/10.1177/0734242X14525822

Dai, S., Li, H., Yang, Z., Dai, M., Dong, X., Ge, X., Sun, M., & Shi, L. (2018). Effects of biochar amendments on speciation and bioavailability of heavy metals in coal-mine-contaminated soil. *Human and Ecological Risk Assessment: An International Journal*, 24(7), 1887–1900. https://doi.org/10.1080/10807039.2018.1429250

Das, D. D., Schnitzer, M. I., Monreal, C. M., & Mayer, P. (2009). Chemical composition of acid–base fractions separated from biooil derived by fast pyrolysis of chicken manure. *Bioresource Technology*, 100(24), 6524–6532. https://doi.org/10.1016/j.biortech.2009.06.104

Das, S. K., Ghosh, G. K., & Avasthe, R. (2020). Biochar application for environmental management and toxic pollutant remediation. *Biomass Conversion and Biorefinery*, 1–12. https://doi.org/10.1007/s13399-020-01078-1

Dieguez-Alonso, A., Funke, A., Anca-Couce, A., Rombolà, A. G., Ojeda, G., Bachmann, J., & Behrendt, F. (2018). Towards biochar and hydrochar engineering – Influence of process conditions on surface physical and chemical properties, thermal stability, nutrient availability, toxicity and wettability. *Energies*, 11(3), 496. https://doi.org/10.3390/en11030496

Figueredo, N. A. D., Costa, L. M. D., Melo, L. C. A., Siebeneichlerd, E. A., & Tronto, J. (2017). Characterization of biochars from different sources and evaluation of release of nutrients and contaminants. *Revista Ciência Agronômica*, 48, 3–403. https://doi.org/10.5935/1806-6690.20170046

Fu, P., Hu, S., Xiang, J., Sun, L., Li, P., Zhang, J., & Zheng, C. (2009). Pyrolysis of maize stalk on the characterization of chars formed under different devolatilization conditions. *Energy and Fuels*, 23(9), 4605–4611. https://doi.org/10.1021/ef900268y

Godwin, P. M., Pan, Y., Xiao, H., & Afzal, M. T. (2019). Progress in preparation and application of modified biochar for improving heavy metal ion removal from wastewater. *Journal of Bioresources and Bioproducts*, 4(1), 31–42. https://doi.org/10.21967/jbb.v4i1.180

Griffin, D. E., Wang, D., Parikh, S. J., & Scow, K. M. (2017). Short-lived effects of walnut shell biochar on soils and crop yields in a long-term field experiment. *Agriculture, Ecosystems and Environment*, 236, 21–29. https://doi.org/10.1016/j.agee.2016.11.002

He, Z., & Ohno, T. (2012). Fourier transform infrared and fluorescence spectral features of organic matter in conventional and organic dairy manure. *Journal of Environmental Quality*, 41(3), 911–919. https://doi.org/10.2134/jeq2011.0226

Herath, I., Kumarathilaka, P., Al-Wabel, M. I., Abduljabbar, A., Ahmad, M., Usman, A. R., & Vithanage, M. (2016). Mechanistic modeling of glyphosate interaction with rice husk derived engineered biochar. *Microporous and Mesoporous Materials*, 225, 280–288. https://doi.org/10.1016/j.micromeso.2016.01.017

Horák, J., Šimanský, V., Aydin, E., Igaz, D., Buchkina, N., & Balashov, E. (2020). Effects of biochar combined with N-fertilization on soil $CO_2$ emissions, crop yields and relationships with soil properties. *Polish Journal of Environmental Studies*, 29(5), 3597–3609. https://doi.org/10.15244/pjoes/117656

Hossain, M. K., Strezov, V., Chan, K. Y., & Nelson, P. F. (2010). Agronomic properties of wastewater sludge biochar and bioavailability of metals in production of cherry tomato (*Lycopersicon esculentum*). *Chemosphere*, 78(9), 1167–1171. https://doi.org/10.1016/j.chemosphere.2010.01.009

Hou, J., Yu, J., Li, W., He, X., & Li, X. (2022). The Effects of chemical oxidation and high-temperature reduction on surface functional groups and the adsorption performance of biochar for sulfamethoxazole adsorption. *Agronomy*, 12(2), 510. https://doi.org/10.3390/agronomy12020510

Huang, H., Reddy, N. G., Huang, X., Chen, P., Wang, P., Zhang, Y., Huang, Y., Lin, P., & Garg, A. (2021). Effects of pyrolysis temperature, feedstock type and compaction on water retention of biochar amended soil. *Scientific Reports*, 11(1), 1–19. https://doi.org/10.1038/s41598-021-86701-5

Huang, Y. F., Kuan, W. H., Lo, S.L., & Lin, C.F. (2008). Total recovery of resources and energy from rice straw using microwave-induced pyrolysis. *Bioresource technology*, 99(17), 8252–8258. https://doi.org/10.1016/j.biortech.2008.03.026

IBI (2012) Standardized product definition and product testing guidelines for biochar that is used in soil. *International Biochar Initiative*. April 2012.

Ippolito, J. A., Cui, L., Kammann, C., Wrage-Mönnig, N., Estavillo, J. M., Fuertes-Mendizabal, T., Cayuela, M. L., Sigua, G., Novak, J., Spokas, K., & Borchard, N. (2020). Feedstock choice, pyrolysis temperature and type influence biochar characteristics: a comprehensive meta-data analysis review. *Biochar*, 2(4), 421–438. https://doi.org/10.1007/s42773-020-00067-x

Janu, R., Mrlik, V., Ribitsch, D., Hofman, J., Sedláček, P., Bielská, L., & Soja, G. (2021). Biochar surface functional groups as affected by biomass feedstock, biochar composition and pyrolysis temperature. *Carbon Resources Conversion*, 4, 36–46. https://doi.org/10.1016/j.crcon.2021.01.003

Jung, J. M., Oh, J. I., Baek, K., Lee, J., & Kwon, E. E. (2018). Biodiesel production from waste cooking oil using biochar derived from chicken manure as a porous media and catalyst. *Energy Conversion and Management*, 165, 628–633. https://doi.org/10.1016/j.enconman.2018.03.096

Keiluweit, M., Nico, P. S., Johnson, M. G., & Kleber, M. (2010). Dynamic molecular structure of plant biomass-derived black carbon (biochar). *Environmental Science and Technology*, 44(4), 1247–1253. https://doi.org/10.1021/es9031419

Khan, K. Y., Ali, B., Cui, X., Feng, Y., Yang, X., & Stoffella, P. J. (2017). Impact of different feedstocks derived biochar amendment with cadmium low uptake affinity cultivar of pak choi (*Brassica rapa* ssb. *chinensis* L.) on phytoavoidation

of Cd to reduce potential dietary toxicity. *Ecotoxicology and Environmental Safety*, 141, 129–138. https://10.1016/j.ecoenv.2017.03.020

Kiran, Y. K., Barkat, A., Cui, X. Q., Ying, F. E. N. G., Pan, F. S., Lin, T. A. N. G., & Yang, X. E. (2017). Cow manure and cow manure-derived biochar application as a soil amendment for reducing cadmium availability and accumulation by *Brassica chinensis* L. in acidic red soil. *Journal of Integrative Agriculture*, 16(3), pp.725–734. https://doi.org/10.1016/S2095-3119(16)61488-0

Kloss, S., Zehetner, F., Dellantonio, A., Hamid, R., Ottner, F., Liedtke, V., Schwanninger, M., Gerzabek, M. H., & Soja, G. (2012). Characterization of slow pyrolysis biochars: effects of feedstocks and pyrolysis temperature on biochar properties. *Journal of Environmental Quality*, 41(4), 990–1000. https://doi.org/10.1016/j.biombioe.2017.06.024

Kung, C.C., McCarl, B. A., & Chen, C. C. (2014). An environmental and economic evaluation of pyrolysis for energy generation in Taiwan with endogenous land greenhouse gases emissions. *International Journal of Environmental Research and Public Health*, 11(3), 2973–2991. https://doi.org/10.3390/ijerph110302973

Lammers, K., Arbuckle-Keil, G., & Dighton, J. (2009). FT-IR study of the changes in carbohydrate chemistry of three New Jersey pine barrens leaf litters during simulated control burning. *Soil Biology and Biochemistry*, 41(2), 340–347. https://doi.org/10.1016/j.soilbio.2008.11.005

Lee, J. W., Kidder, M., Evans, B. R., Paik, S., Buchanan Iii, A. C., Garten, C. T., & Brown, R. C. (2010). Characterization of biochars produced from cornstovers for soil amendment. *Environmental Science and Technology*, 44(20), 7970–7974. https://doi.org/10.1021/es101337x

Lehmann, J., & Joseph, S. eds. (2015). *Biochar for environmental management: science, technology and implementation*. Routledge.

Lehmann, J., Gaunt, J., & Rondon, M. (2006). Bio-char sequestration in terrestrial ecosystems. *Mitig. Adapt. Strat. Glob. Change,* 11, 395–419. https://doi.org/10.1007/s11027-005-9006-5

Li, F., Shen, K., Long, X., Wen, J., Xie, X., Zeng, X., Liang, Y., Wei, Y., Lin, Z., Huang, W., & Zhong, R. (2016). Preparation and characterization of biochars from *Eichornia crassipes* for cadmium removal in aqueous solutions. *PloS one*, 11(2), e0148132. https://doi.org/10.1371/journal.pone.0148132

Lin, D., Pan, B., Zhu, L., & Xing, B. (2007). Characterization and phenanthrene sorption of tea leaf powders. *Journal of Agricultural and Food Chemistry*, 55(14), 5718–5724. https://doi.org/10.1021/jf0707031

Lin, L., Qiu, W., Wang, D., Huang, Q., Song, Z., & Chau, H.W. (2017). Arsenic removal in aqueous solution by a novel Fe-Mn modified biochar composite: characterization and mechanism. *Ecotoxicology and environmental safety*, 144, 514–521. https://doi.org/10.1016/j.ecoenv.2017.06.063

Liu, Y., He, Z., & Uchimiya, M. (2015). Comparison of biochar formation from various agricultural by-products using FTIR spectroscopy. *Modern Applied Science*, 9(4), 246. http://dx.doi.org/10.5539/mas.v9n4p246

Matin, N. H., Jalali, M., Antoniadis, V., Shaheen, S. M., Wang, J., Zhang, T., Wang, H., & Rinklebe, J. (2020). Almond and walnut shell-derived biochars affect sorption-desorption, fractionation, and release of phosphorus in two different soils. *Chemosphere*, 241, 124888. https://doi.org/10.1016/j.chemosphere.2019.124888

Meng, J., Wang, L., Liu, X., Wu, J., Brookes, P. C., & Xu, J. (2013). Physicochemical properties of biochar produced from aerobically composted swine manure and its potential use as an environmental amendment. *Bioresource Technology*, 142, 641–646. https://doi.org/10.1016/j.biortech.2013.05.086

Mochidzuki, K., Soutric, F., Tadokoro, K., Antal, M. J., Tóth, M., Zelei, B., & Várhegyi, G. (2003). Electrical and physical properties of carbonized charcoals. *Industrial and Engineering Chemistry Research*, 42(21), 5140–5151. https://doi.org/10.1021/ie030358e

Mukherjee, A., & Lal, R. (2013). Biochar impacts on soil physical properties and greenhouse gas emissions. *Agronomy*, 3(2), 313–339. https://doi.org/10.3390/agronomy3020313

Novak, J. M., Lima, I., Xing, B., Gaskin, J. W., Steiner, C., Das, K. C., Ahmedna, M., Rehrah, D., Watts, D. W., Busscher, W. J., & Schomberg, H. (2009). Characterization of designer biochar produced at different temperatures and their effects on a loamy sand. *Ann. Environ. Sci*, 3(2), 195–206. https://openjournals.neu.edu/aes/journal/article/view/v3art5

Özçimen, D., & Ersoy-Meriçboyu, A. (2010). Characterization of biochar and bio-oil samples obtained from carbonization of various biomass materials. *Renewable Energy*, 35(6), 1319–1324. https://doi.org/10.1016/j.renene.2009.11.042

Pütün, A. E., Özbay, N., Önal, E. P., & Pütün, E. (2005). Fixed-bed pyrolysis of cotton stalk for liquid and solid products. *Fuel Processing Technology*, 86(11), 1207–1219. https://doi.org/10.1016/j.fuproc.2004.12.006

Rao, H. J. (2021). Characterization studies on adsorption of lead and cadmium using activated carbon prepared from waste tyres. *Nature Environment and Pollution Technology*, 20(2). https://doi.org/10.46488/NEPT.2021.v20i02.012

Regmi, A., Singh, S., Moustaid-Moussa, N., Coldren, C., & Simpson, C. (2022). The Negative Effects of High Rates of Biochar on Violas Can Be Counteracted with Fertilizer. *Plants*,11(4), 491. https://doi.org/10.3390/plants11040491

Sahoo, K., Kumar, A., & Chakraborty, J.P. (2021). A comparative study on valuable products: bio-oil, biochar, non-condensable gases from pyrolysis of agricultural residues. *Journal of Material Cycles and Waste Management*, 23(1), 186–204. https://doi.org/10.1007/s10163-020-01114-2

Septien, S., Valin, S., Dupont, C., Peyrot, M., & Salvador, S. (2012). Effect of particle size and temperature on woody biomass fast pyrolysis at high temperature (1000–1400 C). *Fuel*, 97, 202–210. https://doi.org/10.1016/j.fuel.2012.01.049

Shackley, S., Carter, S., Knowles, T., Middelink, E., Haefele, S., Sohi, S., Cross, A., & Haszeldine, S. (2012). Sustainable gasification-biochar systems? A case-study of rice-husk gasification in Cambodia, Part I: Context, chemical properties, environmental and health and safety issues. *Energy Policy*, 42, 49–58. https://doi.org/10.1016/j.enpol.2011.11.026

Song, H., Wang, J., Garg, A., Lin, X., Zheng, Q., & Sharma, S. (2019). Potential of novel biochars produced from invasive aquatic species outside food chain in removing ammonium nitrogen: Comparison with conventional biochars and clinoptilolite. *Sustainability*, 11(24), 7136. https://doi.org/10.3390/su11247136

Spokas, K. A., Koskinen, W. C., Baker, J. M., & Reicosky, D. C. (2009). Impacts of woodchip biochar additions on greenhouse gas production and sorption/degradation of two herbicides in a Minnesota soil. *Chemosphere*, 77(4), 574–581. https://doi.org/10.1016/j.chemosphere.2009.06.053

Sun, K., Ro, K., Guo, M., Novak, J., Mashayekhi, H., & Xing, B. (2011). Sorption of bisphenol A, 17α-ethinyl estradiol and phenanthrene on thermally and hydrothermally produced biochars. *Bioresource Technology*, 102(10), 5757–5763. https://doi.org/10.1016/j.biortech.2011.03.038

Sun, Y., Gao, B., Yao, Y., Fang, J., Zhang, M., Zhou, Y., Chen, H., & Yang, L. (2014). Effects of feedstock type, production method, and pyrolysis temperature on biochar and hydrochar properties. *Chemical Engineering Journal*, 240, 574–578. https://doi.org/10.1016/j.cej.2013.10.081

Toková, L., Igaz, D., Horák, J., & Aydin, E. (2020). Effect of biochar application and re-application on soil bulk density, porosity, saturated hydraulic conductivity, water content and soil water availability in a silty loam Haplic Luvisol. *Agronomy*, 10(7), 1005. https://doi.org/10.3390/agronomy10071005

Tong, X. J., Li, J. Y., Yuan, J. H., & Xu, R. K. (2011). Adsorption of Cu (II) by biochars generated from three crop straws. *Chemical Engineering Journal*, 172(2–3), 828–834. https://doi.org/10.1016/j.cej.2011.06.069

Trazzi, P. A., Leahy, J. J., Hayes, M. H., & Kwapinski, W. (2016). Adsorption and desorption of phosphate on biochars. *Journal of Environmental Chemical Engineering*, 4(1), 37–46. https://doi.org/10.1007/s12517-021-06629-y

Uchimiya, M., Orlov, A., Ramakrishnan, G., & Sistani, K. (2013). In situ and *ex situ* spectroscopic monitoring of biochar's surface functional groups. *Journal of Analytical and Applied Pyrolysis*, 102, 53–59. https://doi.org/10.1016/j.jaap.2013.03.014

Uchimiya, M., Wartelle, L. H., Klasson, K. T., Fortier, C. A., & Lima, I. M. (2011). Influence of pyrolysis temperature on biochar property and function as a heavy metal sorbent in soil. *Journal of Agricultural and Food Chemistry*, 59(6), 2501–2510. https://doi.org/10.1021/jf104206c

Van de Velden, M., Baeyens, J., Brems, A., Janssens, B., & Dewil, R. (2010). Fundamentals, kinetics and endothermicity of the biomass pyrolysis reaction. *Renewable Energy*, 35(1), 232–242. https://doi.org/10.1016/j.renene.2009.04.019

Verheijen, F., Jeffery, S., Bastos, A. C., Van der Velde, M., & Diafas, I. (2010). Biochar application to soils. A critical scientific review of effects on soil properties, processes, and functions. *EUR*, 24099, 162. https://doi.org/10.2788/472

Wu, W., Yang, M., Feng, Q., McGrouther, K., Wang, H., Lu, H., & Chen, Y. (2012). Chemical characterization of rice straw-derived biochar for soil amendment. *Biomass and bioenergy*, 47, 268–276. https://doi.org/10.1016/j.biombioe.2012.09.034

Xu, Y., Luo, G., He, S., Deng, F., Pang, Q., Xu, Y., & Yao, H. (2019). Efficient removal of elemental mercury by magnetic chlorinated biochars derived from co-pyrolysis of Fe $(NO_3)$ 3-laden wood and polyvinyl chloride waste. *Fuel*, 239, 982–990. https://doi.org/10.1016/j.fuel.2018.11.102

Yaashikaa, P. R., Kumar, P. S., Varjani, S., & Saravanan, A., (2020). A critical review on the biochar production techniques, characterization, stability and applications for circular bioeconomy. *Biotechnology Reports*, 28, e00570. https://doi.org/10.1016/j.btre.2020.e00570

Yaman, S. (2004). Pyrolysis of biomass to produce fuels and chemical feedstocks. *Energy Conversion and Management*, 45(5), 651–671. https://doi.org/10.1016/S0196-8904(03)00177-8

Yang, H., Yan, R., Chen, H., Lee, D. H., & Zheng, C. (2007). Characteristics of hemicellulose, cellulose and lignin pyrolysis. *Fuel*, 86(12–13), 1781–1788. https://doi.org/10.1016/j.fuel.2006.12.013

Yuan, J. H., Xu, R. K., & Zhang, H. (2011). The forms of alkalis in the biochar produced from crop residues at different temperatures. *Bioresource technology*, 102(3), 3488–3497. https://doi.org/10.1016/j.biortech.2010.11.018

Yuan, T., Tahmasebi, A., & Yu, J. (2015). Comparative study on pyrolysis of lignocellulosic and algal biomass using a thermogravimetric and a fixed-bed reactor. *Bioresource Technology*, 175, 333–341. https://doi.org/10.1016/j.biortech.2014.10.108

Zanzi, R., Sjöström, K., & Björnbom, E. (1996). Rapid high-temperature pyrolysis of biomass in a free-fall reactor. *Fuel*, 75(5), 545–550. https://doi.org/10.1016/0016-2361(95)00304-5

Zeng, Z., Ye, S., Wu, H., Xiao, R., Zeng, G., Liang, J., Zhang, C., Yu, J., Fang, Y., & Song, B. (2019). Research on the sustainable efficacy of g-MoS2 decorated biochar nanocomposites for removing tetracycline hydrochloride from antibiotic-polluted aqueous solution. *Science of the Total Environment*, 648, 206–217. https://doi.org/10.1016/j.scitotenv.2018.08.108

Zhang, J., Huang, B., Chen, L., Li, Y., Li, W., & Luo, Z. (2018). Characteristics of biochar produced from yak manure at different pyrolysis temperatures and its effects on the yield and growth of highland barley. *Chemical Speciation and Bioavailability*, 30(1), 57–67. https://doi.org/10.1080/09542299.2018.1487774

Zhang, X., Zhao, B., Liu, H., Zhao, Y., & Li, L. (2022). Effects of pyrolysis temperature on biochar's characteristics and speciation and environmental risks of heavy metals in sewage sludge biochars. *Environmental Technology & Innovation*, 26, 102288. https://doi.org/10.1016/j.eti.2022.102288

Zhao, S. X., Ta, N., & Wang, X. D. (2017). Effect of temperature on the structural and physicochemical properties of biochar with apple tree branches as feedstock material. *Energies*, 10(9), 1293. https://doi.org/10.3390/en10091293

Zolfi Baariani, M., Ronaghi, A., & Ghasemi, R. (2019). Influence of pyrolysis temperatures on FTIR analysis, nutrient bioavailability, and agricultural use of poultry manure biochars. *Communications in Soil Science and Plant Analysis*, 50(4), 402–411. https://doi.org/10.1080/00103624.2018.1563101